Published in final edited form as:
Exp Cell Res. 2010 July 1; 316(11): 1773–1783. doi:10.1016/j.yexcr.2010.02.005.

Neuroprotective Effect of the Endogenous Neural Peptide Apelin in Cultured Mouse Cortical Neurons

Xiang Jun Zeng[1,2], **Shan Ping Yu**[2], **Like Zhang**[1], and **Ling Wei**[2]

[1]Department of Pathophysiology, Capital Medical University, Beijing, China 100069

[2]Department of Anesthesiology, Emory University School of Medicine, Atlanta, GA 30322, USA

Abstract

The adipocytokine apelin and its G protein-coupled APJ receptor were initially isolated from a bovine stomach and have been detected in the brain and cardiovascular system. Recent studies suggest that apelin can protect cardiomyocytes from ischemic injury. Here, we investigated the effect of apelin on apoptosis in mouse primary cultures of cortical neurons. Exposure of the cortical cultures to a serum-free medium for 24 hrs induced nuclear fragmentation and apoptotic death; apelin-13 (1.0 – 5.0 nM) markedly prevented the neuronal apoptosis. Apelin neuroprotective effects were mediated by multiple mechanisms. Apelin-13 reduced serum deprivation (SD)-induced ROS generation, mitochondria depolarization, cytochrome c release and activation of caspase-3. Apelin-13 prevented SD-induced changes in phosphorylation status of Akt and ERK1/2. In addition, apelin-13 attenuated NMDA-induced intracellular Ca^{2+} accumulation. These results indicate that apelin is an endogenous neuroprotective adipocytokine that may block apoptosis and excitotoxic death via cellular and molecular mechanisms. It is suggested that apelins may be further explored as a potential neuroprotective reagent for ischemia-induced brain damage.

Keywords

Cortical neurons; Apelin; Serum deprivation; Apoptosis

Introduction

The APJ is a putative receptor protein with seven-transmembrane domains related to the angiotensin receptor AT1, which is an orphan G protein-coupled receptor cloned from a human genomic library (O'Dowd et al. 1993). The peptide apelin, initially isolated from a bovine stomach, is the endogenous ligand for the APJ receptor (O'Dowd et al. 1993). Apelin is derived from a 77 amino acids length preproapelin that can be cleaved into active apelins containing 13, 17 or 36 amino acids by angiotensin-converting enzyme 2. The most widely studied apelins are apelin-13 and apelin-36. The 13 C-terminal amino acids are completely conserved across all species (Lee et al. 2000). Moreover, apelin-13 invariably exhibits greater degrees of biological potency, including cardiomyocytes protection, than apelin-36 (Simpkin et al. 2007), which advised us to focus on apelin-13 in this investigation. Apelins

Corresponding author: Ling Wei, MD, Department of Anesthesiology, 101 Woodruff Circle, Suite 617, Emory University School of Medicine, Atlanta, GA 30322, Tel. 404-712-8661, Fax 404-712-1351, lwei7@emory.edu.

are widely distributed in various organs and tissues, including the lungs, testis, uterus, and are highly expressed in the cardiovascular system (Kawamata et al. 2001; Kleinz and Davenport 2004; Medhurst et al. 2003). Apelin and its receptor are also abundantly expressed in the brain, detected in many regions of the brain (Lee et al. 2000; Matsumoto et al. 1996; O'Carroll et al. 2000; O'Dowd et al. 1993). They are highly expressed in neurons and oligodendrocytes, and at lower levels in astrocytes (Choe et al. 2000). The hypothalamus represents the major site of apelin-positive nerve fibers. Fibers are also found innervating other circumventricular organs such as the vascular organ of the lamina terminalis, the subfornical and the subcommissural organs and the area postrema. The topographical distribution of apelinergic neurons in the brain suggests multiple roles for apelin such as in the central control of ingestive behaviors, pituitary hormone release, circadian rhythms and body fluid homeostasis (Reaux et al. 2001; Reaux et al. 2002; Takayama et al. 2008). The coexistence of apelin and arginine vasopressin (AVP) in magnocellular neurons and their opposite biological effects support that they are likely to play a key role in maintaining body fluid homeostasis (De Mota et al. 2004). Besides the neuroendocrine functions of apelin (Llorens-Cortes and Kordon 2008), a few recent reports show it is protective against NMDA-mediated excitotoxicity in hippocampal neurons and suppresses apoptosis in human osteoblasts (O'Donnell et al. 2007; Xie et al. 2007), which may depend on the phosphatidylinositol-3 kinase (PI3K) pathway. More recent studies demonstrate that apelin-13 is protective against ischemia-induced injury in cardiomyocytes (Falcao-Pires et al. 2009; Zeng et al. 2009).

Neuronal cell death is a feature of acute and chronic neurodegenerative diseases that occurs mainly by necrosis and apoptosis (Lipton 1999; Mattson 2000; Yuan et al. 2003). Cortical neurons deprived of serum undergo typical apoptosis, mediated by caspase-dependent and caspase-independent pathways (Chauvier et al. 2005; Wei et al. 2004a). ROS generation, mitochondrial depolarization, cytochrome crelease and caspase activation play important roles in the SD-induced neuronal apoptosis (Chauvier et al. 2005). In addition, inhibited PI3K and increased extracellular signal-regulated MAPK (ERK1/2) have been linked to SD-induced neuronal apoptosis (Chang et al. 2004). We hypothesized that activation of the APJ receptor by apelin-13 might abolish the mitochondrial dysfunction through PI3K and ERK1/2 pathways.

Experimental Procedures

Preparation of mouse pure cortical neurons

Primary mouse cortical cultures were prepared from embryonic day 16 Swiss Webster mice as previously described with minor modifications (Wang and Yu 2005). Briefly, the cerebral cortical regions from embryonic day 16 (E16) mouse fetuses were dissected in ice-cold Ca^{2+}/Mg^{2+}-free Hanks' salt solution (HSS), pH 7.5. After removal of the meninges, cells were dissociated by a mild trypsinization (0.25%) (Invitrogen, Carlsbad, CA) followed by gently blowing through an autoclaved pipette. The cells were then plated at a density of 1×10^6 cells on 3.5-cm dishes pre-coated with poly-L-ornithine (0.1 mg/ml, Sigma, St. Louis, MO) and laminin (1mg/ml, Sigma). The culture medium of 10% horse serum in media stock (MS) was changed to Neurobasal-medium (Invitrogen) supplemented with B27 (Invitrogen) and L-glutamine (0.5 mM, Invitrogen) the next day. Cytosine arabinoside was added into the medium (1 μM final concentration) at the third day to inhibit astrocytes proliferation. The cells were cultured at 37°C in a humidified atmosphere of 5% CO_2 and 95% air and were used at 7 days in vitro (DIV). The cortical cultures contain mostly neurons and there were <2% glial cells as determined by immunohistochemical staining.

Western blotting of protein expression in cortical neurons

Cortical cultures were exposed to sham wash or SD with or without apelin-13. More experimental groups included apelin-13 plus specified treatment. After treatments, 40 μg cell lysate was subjected to sodium dodecyl sulfate–polyacrylamide gel electrophoresis. The gel was blotted onto a PVDF membrane (Millipore, Bedford, MA) and the filters were blocked with 5% BSA /0.05% Tween/PBS, followed by overnight incubation at 4°C with primary antibody in 5% BSA /0.05% Tween/PBS. The primary antibodies used were as follows: rabbit anti-APJ (Santa Cruz Biotechnology, Inc, CA), goat anti-caspase-3, mouse anti-β-actin (Sigma), mouse anti-VDAC, mouse anti-cytochrome C, rabbit anti-p-AKT (Thr308), rabbit anti-AKT, rabbit anti-ERK-1/2-P, rabbit anti-ERK-1/2, and rabbit anti-tubulin (Cell Signaling Technology; Danvers, MA). The membrane was washed 3 times with 0.05% tween/PBS and incubated with alkaline phosphatase -conjugated secondary antibody (Cell Signaling Technology) at a 1:2000 dilution (5% BSA /0.05% Tween/PBS; 1 hr at room temperature), rewashed for 3 times and the membranes were developed by the addition of BCIP/NBT solution (Sigma). The membrane was scanned and analyzed by densitometry using Adobe Photoshop (Adobe Systems Inc., San Jose, CA) and Image J (NIH, Bethesda, MD). Signal intensities of phosphorylated or activated proteins were normalized to α-tubulin.

Immunohistochemical staining

For immunofluorescent imaging, the cultured cells were fixed with 100% methanol for 5min, then in ethanol:acetic (2:1) solution for 5 min, and permeabilizing cells with 0.2% tritonX-100. After blocking with 1% fish gel in PBS for 1 hr at room temperature, the primary antibody was added and incubated at 4°C overnight. Rabbit anti-APJ polyclonal antibody (APJR-1, Santa Cruz Biotechnology, Inc) was diluted into 2 μg/ml in PBS, mouse anti-NeuN monoclonal antibody (1 mg/ml, Chemicon, Millipore Corporation) was diluted into 2.5 μg/ml in PBS. The next day, the dishes were washed with PBS three times, then incubated for 2 hrs at room temperature with secondary antibodies diluted with PBS. Secondary antibodies include Alexa Fluor 488 goat anti—mouse IgG (2 mg/ml, Invitrogen), diluted into 10 μg/ml, donkey anti-Rabbit IgG Polyclonal antibody and Cy3 conjugate (500 μg, Chemicon, Millipore Corporation) diluted into 1 μg/ml. After washing with PBS three times, Hoechst 33342 (1:20000 in PBS; Molecular Probes, Carlsbad, CA) was added and incubated for 5min followed with PBS wash for 3 times. Coverslips were mounted on the bottom of the dishes in VECTASHIELD Fluorescent Mounting Media (10 ml, Vector Laboratories, Inc., Burlingame, CA). Micrographs were captured on an Olympus IX61 microscope at 80X.

Cell death assay in primary cortical neurons

In control experiments of testing cytotoxicity induced by apelin, cortical neurons were incubated with different concentrations of apelin-13 (Sigma) in culture medium for 24 hrs, trypan blue were then added into the medium and incubated at 37°C for 15 min before counting total and trypan blue positive cells under a light microscope in five fields per dish. At least three dishes were examined for every apelin-13 concentration. In serum deprivation experiments, primary cortical cultures of 7 days in vitro (DIV) were washed with B27- and L-glutamine-free neurobasal medium for 5 times and exposed to this medium for 24 hrs. DIV 7 neuronal cultures were used because younger cells are more sensitive to apoptosis. In neuroprotective assay, apelin-13 (10 pM - 5nM, Sigma) was co-applied into the medium. The percentage of dead cortical neurons was analyzed by counting the trypan blue positive neurons versus total neurons. In addition, Hoechst 33342 staining of shrunken nuclei was used to confirm the apoptotic nature of the cell death.

In excitotoxicity experiments, the effect of apelin-13 on NMDA-induced cell death in cortical neurons of 12 DIV was tested. DIV 12 cortical cultures were used based on the well-known fact that functional NMDA receptors in cortical neurons are well developed after 10–12 days in culture. Cortical neurons were washed with neurobasal medium 5 times, then NMDA (30 μM) with and without apelin-13 (0.1 nM – 5 nM) was added into the medium. After 24 hrs, release of lactate dehydrogenase (LDH) into the medium was detected using a cytotoxicity LDH detection kit (Roche, Nutley, NJ), according to the user manual. Briefly, 50 μl medium and 50 μl mixture of reagent A and B were co-incubated for 30 min and then detected the absorbance at 492 nm with a spectrophotometer (Sunrise Instruments, LLC **,**Hebron, NH). The results were normalized to the basal LDH release in control cultures.

Terminal deoxynucleotidyltransferase-mediated DUTP-biotin nick end labeling (TUNEL) staining

DNA damage and cell death were measured using a DeadEnd™ Fluorometric TUNEL detection System (G3250, Promega Corporation, Madison, WI). The day before TUNEL assay, cortical neurons were stained with NeuN, the secondary antibody was donkey anti-mouse IgG polyclonal antibody, Cy3 conjugate (500 μg, AP192C, Chemicon) diluted into 1μg/ml. After NeuN staining, TUNEL staining was performed according to the user protocol. Briefly, cells were equilibrated with Buffer for 10 min and incubated in rTdT Incubation Buffer for 60 min at 37°C, then in 2×SSC for 15 min at room temperature, followed by Hoechst 33342 (1:20000) staining for 5 min. The dishes were mounted in VECTASHIELD Mounting Medium (Vector Laboratories, Inc). TUNEL and NeuN double stained cells were quantified by counting cells in five non-overlapping fields captured under an Olympus IX61 microscope at 20×, and the double positive cells were counted, the ratio of NeuN positive cells among total cells (Hoechst 33342 positive cells) was calculated.

Caspase-3 activation assay

Caspase-3 activation was measured using immunostaining and the antibody against the active form of caspase-3 16 hrs after serum deprivation. Briefly, cortical neurons were fixed with 10% formalin and permeabilized with 0.2% tritonX-100, then blocked with 1% fish gel, followed by incubation at 4°C overnight with primary antibodies: rabbit anti-cleaved caspase-3 poly antibody (1:200, Chemicon) and mouse anti-NeuN monoclonal antibody (1:400, Chemicon). The dishes were balanced at room temperature for 1 hr, then incubate with secondary antibodies: donkey anti-rabbit488 (1:200, A21206, Invitrogen), donkey anti-mouse IgG polyclonal antibody, Cy3 (1:1000, Chemicon). The dishes were mounted in VECTASHIELD Mounting Medium (Vector Laboratories, Inc). Caspase-3 and NeuN double stained cells and NeuN-positive cells were quantified and averaged by counting cells in five non overlapping fields captured on an Olympus IX61 microscope at 20×, at least 1000 NeuN positive cells were counted.

Fluorescent imaging of the mitochondria membrane potential

Mitochondrial membrane potential (Δψm) was inspected in cortical neurons using the fluorescent indicator tetramethylrhodamine methyl-ester perchlorate (TMRM, Invitrogen). TMRM (30 nM) was loaded for 30 min at 37°C in the dark, and the cells were then washed with fresh medium and treated with serum deprivation with or without apelin-13 for 10 hrs. Fluorescent emission was excited at 543 nM. TMRM fluorescence was measured using a fluorescence microscope (Nikon TE2000S, New York). The quantification of the fluorescent intensity was done using the Image J software (NIH, Baltimore, MD).

Detection of the reactive oxygen species (ROS) in cortical neurons

Dihydroethidium (DHE) (Molecular Probes, Eugene, OR) was prepared in DMSO and the stock solution was further diluted in culture medium before testing. After experimental treatments, the cells were incubated with 5 μml/L DHE in culture medium for 5 min at 37°C in the dark, and fluorescence images were taken to count the DHE positive nuclei of cells. Three independent experiments were performed. Five fields in every experiment were taken, and the percentage of DHE positive cells to total cells was calculated.

Isolate mitochondria from primary cortical neurons

Mitochondrial and cytosol fractions were isolated to detect cytochrome c distribution using the Mitochondria Isolate Kit for cultured cells (Pierce, IL). Briefly, reagents were added in order and centrifuged, after transfer the cytosol fraction the pellet containing the isolated mitochondria was washed and centrifuged again, and then lysis buffer was added and centrifuged to get the mitochondrial protein.

Calcium measurement in cortical neurons

Fluorescent confocal microscopy (Zeiss LSM5 PASCAL laser scanning confocal microscope, Carl Zeiss, Germany) and the Ca^{2+} dye fluo-4 were used to detect calcium concentration changes in cortical neurons. Briefly, cortical neurons were pre-incubated for 30 min with fluo-4-AM (Invitrogen); the medium was then changed into a fresh Neurobasal-medium and incubated for another 30 min. After 50 μM NMDA treatment with or without apelin in the medium fluo-4 fluorescence intensity of similar populations of cells was detected for 20 min, and the fluorescent density was analyzed using Image J (NIH).

Statistical analyses

Comparisons were made using one-way ANOVA. All experiments were repeated at least three times. Alterations are judged significant when the *P* values are less than 0.05. Data are presented as the mean ± SEM.

Results

Expression of APJ in cortical neurons

We first examined the protein expression of APJ in primary cultured mouse cortical neurons using Western blot and immunochemical staining with a polyclonal anti-APJ antibody (Fig. 1). Withdrawal of serum from the culture medium (24 hrs) did not significantly alter the APJ expression (Fig. 1D). Many APJ-positive cells are NeuN staining positive, suggesting the APJ expression in cultured cortical neurons. APJ expression was also observed in glial cells (data not show).

Effects of apelin-13 on mitochondrial dysfunction, ROS production, and apoptosis in cortical neurons

Both apoptosis and necrosis can cause mitochondrial depolarization and increased ROS production. To selectively test the role of apelin-13 in apoptotic cells, we used the typical apoptotic insult serum deprivation. Serum withdrawal caused marked mitochondrial depolarization assessed using the TMRM fluorescent dye (Fig. 2). Apelin-13 showed a substantial ability for maintaining the polarized mitochondrial membrane potential, there was little depolarization when apelin-13 (5 nM) was added into the serum-free medium (Fig. 2). The mitochondrial compartment is a main source for generation of ROS. In line with its ability to maintain mitochondrial potential, apelin-13 (0.5 and 5.0 nM) significantly reduced ROS production in cortical neurons undergoing SD treatment (Fig. 3).

Consistent with the apoptotic nature of SD-induced neuronal cell death, there was a significant cytochrome c release from the mitochondria into cytosol. Co-applied apelin-13 in serum-free medium dose-dependently (0.1 – 1.0 nM) prevented cytochrome c release measured by the cytochrome c content in mitochondrial and cytosol compartments using Western blot analysis (Fig. 4). In the presence of 0.5 and 5 nM apelin-13, the mitochondrial cytochrome c was even higher than in control cells, the mechanism of this event is unclear. Apelin-13 also substantially prevented caspase-3 activation assessed 16 hrs following the onset of SD treatment (Fig. 5).

Consistent with above observations, SD-induced cell death measured by TUNEL staining, condensed nuclei and trypan blue staining was attenuated by co-applied apelin-13 in a concentration-dependent manner from 0.5 to 5.0 nM (Fig. 6). At 1.0 nM, apelin-13 reduced the number of TUNEL positive cells from 55 ± 2% of total neurons in SD group to 33 ± 3% in SD plus apelin group ($p < 0.05$). Apelin-13 at 5 nM showed the strongest neuroprotection (~40% reduction in cell death); even higher concentration of apelin-13 did not display additional effect.

Role of Akt and ERK1/2 signaling in apelin-13 effect

Wortmannin is a selective inhibitor of the phosphatidylinositol-3-kinase (PI3K)/Akt signaling pathway. Co-applied wortmannin (1.0 μM) eliminated the neuroprotective effect of apelin-13, suggesting that the PI3K/Akt pathway could mediate the apelin-13 effect (Fig. 6). Wortmannin alone did not display toxic effects on cortical cells (Fig. 6). To further explore the signaling pathways that participate in the apelin effects, we measured phosphorylation levels of ERK1/2 and Akt after SD. Withdrawal of serum increased ERK1/2 phosphorylation while apelin attenuated this SD-induced effect (Fig 7). Conversely, 4 hrs into SD the Akt phosphorylation level decreased while co-applied apelin-13 prevented this phosphorylation decrease (Fig. 7).

Apelin-13 protects cortical neurons against NMDA-induced excitotoxicity

The next experiment was performed to test whether apelin-13 might be able to protect central neurons against excitotoxicity that takes place after cerebral ischemia. Cultured cortical neurons were exposed to NMDA (30 μM) and cell death was measured 24 hrs later by LDH release. Again, apelin-13 (0.1 – 5 nM) co-applied with NMDA showed marked neuroprotection in a concentration-dependent manner (Fig. 8).

Since activation of NMDA receptors mediates a large Ca^{2+} influx that is believed responsible for excitotoxicity, we tested the idea that apelin-13 might show inhibitory actions on NMDA-triggered intracellular Ca^{2+} increases. Using the fluorescent dye fluo-4 and confocal imaging, NMDA (50 μM, 10 min) triggered a 3-fold enhancement in fluorescence intensity while this increase was largely eliminated by co-applied apelin-13 (5 nM) (Fig. 8).

Discussion

The aim of this study was to evaluate the neuroprotective effect and mechanism of the endogenous APJ receptor peptide ligand apelin against neuronal apoptosis in cultured mouse cortical neurons. Multiple assessments demonstrate concentration-dependent neuroprotective effects of apelin-13 against serum deprivation-induced apoptosis. Apelin-13 not only blocks typical apoptosis, it also shows inhibitory effect on NMDA-induced intracellular Ca^{2+} increases and excitotoxicity. Various mechanisms may mediate apelin-induced neuroprotection, these include inhibition on apoptotic cascade, protection of

mitochondria membrane potential and mitochondrial function, maintenance of Ca^{2+} homeostasis and phosphorylation states of PI3/Akt/ERK1/2 pathways.

A recent paper showed that apelin protected hippocampal neurons against NMDA receptor-mediated excitotoxicity (O'Donnell et al. 2007). The effect was likely mediated by the phosphorylation of Akt and Raf/ERK1/2 in these neurons. It was concluded that apelin/APJ signaling likely represents an endogenous hippocampal neuronal survival response, and therefore apelin should be further investigated as a potential neuroprotectant against hippocampal injury. On the contrary, some studies could not identify the involvement of the PI3K/Akt pathway in apelin induced myocardial protection (Kleinz and Baxter 2008). It was suggested that signaling pathways other than Akt/ERK1/2 genes might participate in apelin effects. This speculation, however, remains to be supported by experimental evidence. The present investigation supports the role of the PI3K/Akt pathway in the neuroprotective effect of apelin in cortical neurons. Increased generation of ROS is a major injurious mechanism in serum deprivation induced cell death (Zhuge and Cederbaum 2006). We show that apelin is a potent antagonist against ROS production. Moreover, we show that apelin is highly effective in preventing a cascade of apoptotic events and apoptotic death in these neurons. This is consistent with recent investigations that apelin can ameliorate apoptosis in the rat's heart and human osteoblasts (Xie et al. 2007; Zeng et al. 2009).

In the present investigation, we identified the protein expression of apelin and APJ receptor in cortical neurons. Our data support an endogenous neuroprotective role for the apelin/APJ system in central neurons. The neuroprotective action of APJ receptor activation significantly reduces not only typical apoptosis but also the excitotoxic cell death that is likely consisted of both apoptotic and necrotic components (Wei et al. 2004b). Consistent with the anti-apoptotic property of apelin, it shows marked block on mitochondrial dysfunction, cytochrome c release, ROS production, and caspase activation. Supporting its protection against excitotoxicity, apelin significantly attenuates intracellular Ca^{2+} accumulation. This observation is in line with the report that apelin protected hippocampus neurons from the excitotoxic insult induced by quinolinic acid (O'Donnell et al. 2007). The quinolinic acid induced cell death was blocked by the NMDA receptor antagonist MK801, verifying the mediation of this excitotoxicity by NMDA receptors. That investigation, however, did not provide information on Ca^{2+} homeostasis that is closely associated with excitotoxicity. Although our data demonstrate the inhibitory effect of apelin on NMDA-induced intracellular Ca^{2+} accumulation, whether apelin has a direct inhibitory action on the NMDA receptor activity, i.e. NMDA receptor current, remains to be verified.

The influx of extracellular Ca^{2+} into the cytoplasm via NMDA receptor, followed by Ca^{2+} accumulation in mitochondria, causes a mitochondrial membrane depolarization. The loss of mitochondrial membrane potential changes the membrane permeability of mitochondria. Opening of the permeability transition pore is an important step in the apoptotic process and a previous study showed it could be inhibited by apelin (Simpkin et al. 2007). We examined mitochondrial membrane potential changes in serum deprivation-induce apoptosis with TMRM imaging, whose fluorescence is a direct reflection of the mitochondrial potential. Our results show apelin-13 prevents the loss of mitochondrial membrane potential induced by the apoptotic insult, suggesting the mitochondria protection could be a major action of apelin in blocking apoptosis. A previous investigation showed that apelin alone could induce calcium elevations in human NT2.N neurons (Choe et al. 2000). The Ca^{2+} increase, however, was relatively moderate, much less than that induced by glutamate. In our experiments, we did not observe the Ca^{2+} increase induced by apelin most likely due to lower concentrations used in our experiments (5 nM vs. 120 nM). It is possible that apelin may act as a "partial/weak agonist" of Ca^{2+} influx and competes with glutamate or NMDA, by which the large increase in intracellular Ca^{2+} mediated by NMDA receptors is minimized

when apelin is co-applied with a glutamate agonist. Again, it will be interesting to test a putative action of apelin-13 on NMDA receptors.

PI3K/Akt and ERK1/2 pathways have been linked to neuronal cell survival and/or cell death (Armstrong 2004; Cross et al. 2000; Hetman and Kharebava 2006). Some investigations show that increased PI3K/Akt and/or decreased ERK1/2 phosphorylation are neuroprotective, although some others reported opposite effects (Almeida et al. 2005; Bickler and Fahlman 2006; Jantas and Lason 2009; Niimura et al. 2006). The difference might be at least partly due to cell specific mechanisms. For example, cell protection ensured by activation of the AKT and ERK was observed in the retina; in contrast, their protective effects differed in the brain (Lievens et al. 2008). AKT failed to prevent brain neuronal death and lethality of *Drosophila* . ERK had no beneficial effects in the retina or brain. An increased phosphorylation of ERK1/2 was linked to the formation of ROS in cerebella granule cells (Myhre et al. 2004). It is possible, that ROS induced cell injury would be associated with increased phosphorylation of ERK1/2. Our study confirmed that apelin-13 has marked influences on phosphorylation status of PI3K/Akt and ERK/12 in mouse cortical neurons. Following SD exposure, the level of phosphorylated AKT was decreased and that of ERK1/2 was increased. Apelin dose-dependently increased the phosphorylation of Akt and decrease of ERK1/2 phosphorylation. Consistently, apelin effectively attenuated ROS production. This indicates that the apelin/APJ signaling in cortical neurons changes Akt and ERK1/2 phosphorylation which may mediate the enhanced survival of the cells.

ROS is generated in mitochondrial electron transport system, which can be scavenged by endogenous anti-oxidant systems (Droge 2002). However, when ROS levels exceed the antioxidant capacity of the cell, or when antioxidant systems become deficient, oxidative stress and neuronal damage occurs (Klein and Ackerman 2003). Increased production of ROS has been identified as a major injurious mechanism of neuronal death including serum deprivation-induced apoptosis (Satoh et al. 1996). We tested the hypothesis that apelin could show inhibitory effect on ROS production. Our results illustrated that apelin dose-dependently reduced the formation of ROS in cortical cell cultures. It is suggested that the anti-ROS property of apelin is one of the protective mechanisms of apelin-13. It will be interesting and important to learn whether apelin is able to act as a ROS scavenger or shows inhibitory effect on ROS production in the mitochondria.

Taken together, we propose that apelin-13 may act as an endogenous neuroprotective molecule that can activate multiple protective mechanisms and is able not only prevent typical apoptosis but also antagonizes excitotoxicity. Since both necrosis and apoptosis have been linked to neuronal death after ischemic stroke, trauma, spinal cord injury and some neurodegenerative diseases, apelins should be further explored as an endogenous surviving signal and/or potential treatment under these pathological conditions.

Acknowledgments

This work was supported by NIH grants NS 37372, NS 045155, and NS 045810, and American Heart Association Established Investigator Award.

References

Almeida RD, Manadas BJ, Melo CV, Gomes JR, Mendes CS, Graos MM, Carvalho RF, Carvalho AP, Duarte CB. Neuroprotection by BDNF against glutamate-induced apoptotic cell death is mediated by ERK and PI3-kinase pathways. Cell Death Differ. 2005; 12(10):1329–1343. [PubMed: 15905876]

Armstrong SC. Protein kinase activation and myocardial ischemia/reperfusion injury. Cardiovasc Res. 2004; 61(3):427–436. [PubMed: 14962474]

Bickler PE, Fahlman CS. The inhaled anesthetic, isoflurane, enhances Ca2+-dependent survival signaling in cortical neurons and modulates MAP kinases, apoptosis proteins and transcription factors during hypoxia. Anesth Analg. 2006; 103(2):419–429. table of contents. [PubMed: 16861427]

Chang SH, Poser S, Xia Z. A novel role for serum response factor in neuronal survival. J Neurosci. 2004; 24(9):2277–2285. [PubMed: 14999078]

Chauvier D, Lecoeur H, Langonne A, Borgne-Sanchez A, Mariani J, Martinou JC, Rebouillat D, Jacotot E. Upstream control of apoptosis by caspase-2 in serum-deprived primary neurons. Apoptosis. 2005; 10(6):1243–1259. [PubMed: 16215683]

Choe W, Albright A, Sulcove J, Jaffer S, Hesselgesser J, Lavi E, Crino P, Kolson DL. Functional expression of the seven-transmembrane HIV-1 co-receptor APJ in neural cells. J Neurovirol. 2000; 6(Suppl 1):S61–69. [PubMed: 10871767]

Cross TG, Scheel-Toellner D, Henriquez NV, Deacon E, Salmon M, Lord JM. Serine/threonine protein kinases and apoptosis. Exp Cell Res. 2000; 256(1):34–41. [PubMed: 10739649]

De Mota N, Reaux-Le Goazigo A, El Messari S, Chartrel N, Roesch D, Dujardin C, Kordon C, Vaudry H, Moos F, Llorens-Cortes C. Apelin, a potent diuretic neuropeptide counteracting vasopressin actions through inhibition of vasopressin neuron activity and vasopressin release. Proc Natl Acad Sci U S A. 2004; 101(28):10464–10469. [PubMed: 15231996]

Droge W. Free radicals in the physiological control of cell function. Physiol Rev. 2002; 82(1):47–95. [PubMed: 11773609]

Falcao-Pires I, Goncalves N, Henriques-Coelho T, Moreira-Goncalves D, Roncon-Albuquerque R Jr, Leite-Moreira AF. Apelin decreases myocardial injury and improves right ventricular function in monocrotaline-induced pulmonary hypertension. Am J Physiol Heart Circ Physiol. 2009; 296(6):H2007–2014. [PubMed: 19346461]

Hetman M, Kharebava G. Survival signaling pathways activated by NMDA receptors. Curr Top Med Chem. 2006; 6(8):787–799. [PubMed: 16719817]

Jantas D, Lason W. Different Mechanisms of NMDA-Mediated Protection Against Neuronal Apoptosis: A Stimuli-Dependent Effect. Neurochem Res. 2009

Kawamata Y, Habata Y, Fukusumi S, Hosoya M, Fujii R, Hinuma S, Nishizawa N, Kitada C, Onda H, Nishimura O, Fujino M. Molecular properties of apelin: tissue distribution and receptor binding. Biochim Biophys Acta. 2001; 1538(2–3):162–171. [PubMed: 11336787]

Klein JA, Ackerman SL. Oxidative stress, cell cycle, and neurodegeneration. J Clin Invest. 2003; 111(6):785–793. [PubMed: 12639981]

Kleinz MJ, Baxter GF. Apelin reduces myocardial reperfusion injury independently of PI3K/Akt and P70S6 kinase. Regul Pept. 2008; 146(1–3):271–277. [PubMed: 18022257]

Kleinz MJ, Davenport AP. Immunocytochemical localization of the endogenous vasoactive peptide apelin to human vascular and endocardial endothelial cells. Regul Pept. 2004; 118(3):119–125. [PubMed: 15003827]

Lee HJ, Tomioka M, Takaki Y, Masumoto H, Saido TC. Molecular cloning and expression of aminopeptidase A isoforms from rat hippocampus. Biochim Biophys Acta. 2000; 1493(1–2):273–278. [PubMed: 10978538]

Lievens JC, Iche M, Laval M, Faivre-Sarrailh C, Birman S. AKT-sensitive or insensitive pathways of toxicity in glial cells and neurons in Drosophila models of Huntington's disease. Hum Mol Genet. 2008; 17(6):882–894. [PubMed: 18065778]

Lipton P. Ischemic cell death in brain neurons. Physiol Rev. 1999; 79(4):1431–1568. [PubMed: 10508238]

Llorens-Cortes C, Kordon C. Jacques Benoit lecture: the neuroendocrine view of the angiotensin and apelin systems. J Neuroendocrinol. 2008; 20(3):279–289. [PubMed: 18194430]

Matsumoto M, Hidaka K, Akiho H, Tada S, Okada M, Yamaguchi T. Low stringency hybridization study of the dopamine D4 receptor revealed D4-like mRNA distribution of the orphan seven-transmembrane receptor, APJ, in human brain. Neurosci Lett. 1996; 219(2):119–122. [PubMed: 8971794]

Mattson MP. Apoptosis in neurodegenerative disorders. Nat Rev Mol Cell Biol. 2000; 1(2):120–129. [PubMed: 11253364]

Medhurst AD, Jennings CA, Robbins MJ, Davis RP, Ellis C, Winborn KY, Lawrie KW, Hervieu G, Riley G, Bolaky JE, Herrity NC, Murdock P, Darker JG. Pharmacological and immunohistochemical characterization of the APJ receptor and its endogenous ligand apelin. J Neurochem. 2003; 84(5):1162–1172. [PubMed: 12603839]

Myhre O, Sterri SH, Bogen IL, Fonnum F. Erk1/2 phosphorylation and reactive oxygen species formation via nitric oxide and Akt-1/Raf-1 crosstalk in cultured rat cerebellar granule cells exposed to the organic solvent 1,2,4-trimethylcyclohexane. Toxicol Sci. 2004; 80(2):296–303. [PubMed: 15141098]

Niimura M, Takagi N, Takagi K, Funakoshi H, Nakamura T, Takeo S. Effects of hepatocyte growth factor on phosphorylation of extracellular signal-regulated kinase and hippocampal cell death in rats with transient forebrain ischemia. Eur J Pharmacol. 2006; 535(1–3):114–124. [PubMed: 16516191]

O'Carroll AM, Selby TL, Palkovits M, Lolait SJ. Distribution of mRNA encoding B78/apj, the rat homologue of the human APJ receptor, and its endogenous ligand apelin in brain and peripheral tissues. Biochim Biophys Acta. 2000; 1492(1):72–80. [PubMed: 11004481]

O'Donnell LA, Agrawal A, Sabnekar P, Dichter MA, Lynch DR, Kolson DL. Apelin, an endogenous neuronal peptide, protects hippocampal neurons against excitotoxic injury. J Neurochem. 2007; 102(6):1905–1917. [PubMed: 17767704]

O'Dowd BF, Heiber M, Chan A, Heng HH, Tsui LC, Kennedy JL, Shi X, Petronis A, George SR, Nguyen T. A human gene that shows identity with the gene encoding the angiotensin receptor is located on chromosome 11. Gene. 1993; 136(1–2):355–360. [PubMed: 8294032]

Reaux A, De Mota N, Skultetyova I, Lenkei Z, El Messari S, Gallatz K, Corvol P, Palkovits M, Llorens-Cortes C. Physiological role of a novel neuropeptide, apelin, and its receptor in the rat brain. J Neurochem. 2001; 77(4):1085–1096. [PubMed: 11359874]

Reaux A, Gallatz K, Palkovits M, Llorens-Cortes C. Distribution of apelin-synthesizing neurons in the adult rat brain. Neuroscience. 2002; 113(3):653–662. [PubMed: 12150785]

Satoh T, Sakai N, Enokido Y, Uchiyama Y, Hatanaka H. Survival factor-insensitive generation of reactive oxygen species induced by serum deprivation in neuronal cells. Brain Res. 1996; 733(1): 9–14. [PubMed: 8891242]

Simpkin JC, Yellon DM, Davidson SM, Lim SY, Wynne AM, Smith CC. Apelin-13 and apelin-36 exhibit direct cardioprotective activity against ischemia-reperfusion injury. Basic Res Cardiol. 2007; 102(6):518–528. [PubMed: 17694254]

Takayama K, Iwazaki H, Hirabayashi M, Yakabi K, Ro S. Distribution of c-Fos immunoreactive neurons in the brain after intraperitoneal injection of apelin-12 in Wistar rats. Neurosci Lett. 2008; 431(3):247–250. [PubMed: 18164129]

Wang XQ, Yu SP. Novel regulation of Na, K-ATPase by Src tyrosine kinases in cortical neurons. J Neurochem. 2005; 93(6):1515–1523. [PubMed: 15935067]

Wei L, Xiao AY, Jin C, Yang A, Lu ZY, Yu SP. Effects of chloride and potassium channel blockers on apoptotic cell shrinkage and apoptosis in cortical neurons. Pflugers Arch. 2004a; 448(3):325–334. [PubMed: 15057559]

Wei L, Ying DJ, Cui L, Langsdorf J, Yu SP. Necrosis, apoptosis and hybrid death in the cortex and thalamus after barrel cortex ischemia in rats. Brain Res. 2004b; 1022(1-2):54–61. [PubMed: 15353213]

Xie H, Yuan LQ, Luo XH, Huang J, Cui RR, Guo LJ, Zhou HD, Wu XP, Liao EY. Apelin suppresses apoptosis of human osteoblasts. Apoptosis. 2007; 12(1):247–254. [PubMed: 17136493]

Yuan J, Lipinski M, Degterev A. Diversity in the mechanisms of neuronal cell death. Neuron. 2003; 40(2):401–413. [PubMed: 14556717]

Zeng XJ, Zhang LK, Wang HX, Lu LQ, Ma LQ, Tang CS. Apelin protects heart against ischemia/reperfusion injury in rat. Peptides. 2009; 30(6):1144–1152. [PubMed: 19463748]

Zhuge J, Cederbaum AI. Serum deprivation-induced HepG2 cell death is potentiated by CYP2E1. Free Radic Biol Med. 2006; 40(1):63–74. [PubMed: 16337880]

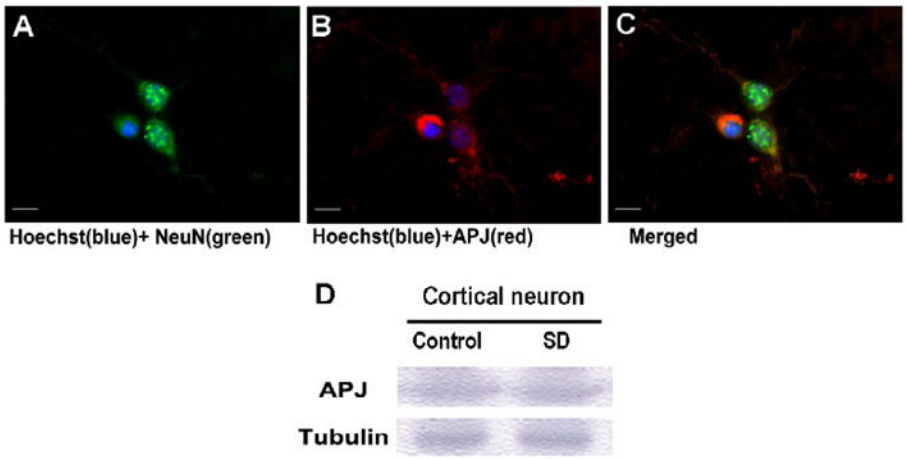

Figure 1. Expression of APJ protein in cortical neurons

Immunohistochemical staining and Western blot were used to detect expression of APJ receptor in cultured cortical neurons of 10-DIV. **A**-**C**. Images show NeuN- and APJ-positive cells and colocalization of these two labels in the merged image. Hoechst 33342 staining illustrates cell nuclei in the imaging field. Scale bar equals to 10 μm. **D**. Western blotting with an anti-APJ polyclonal antibody showed expression of APJ receptor in cortical neurons in control cells and after serum deprivation (SD). The expression level was similar. Tubulin was used as a loading control.

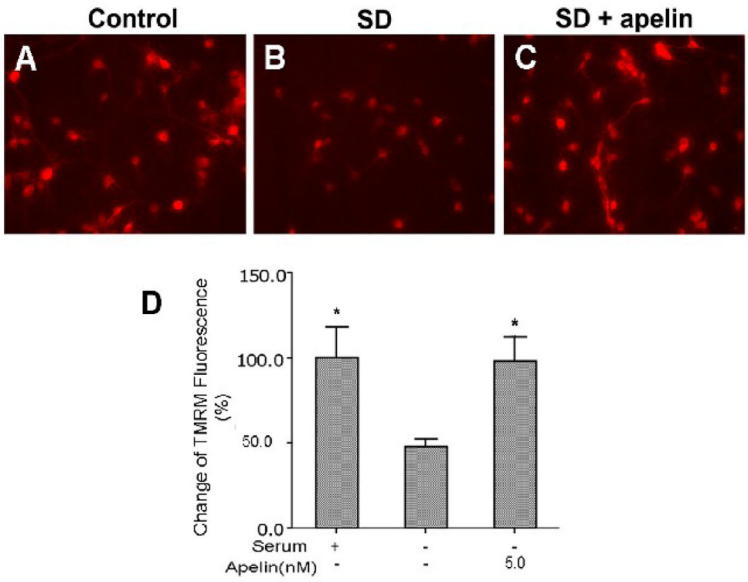

Figure 2. Maintenance of mitochondrial membrane potential by apelin-13 in apoptotic cells

Immunocytochemical imaging using the mitochondrial membrane potential dye TMRM was performed in cortical neuronal cultures. **A** – **C**. TMRM fluorescence was measured 10 hrs after serum deprivation with or without co-applied apelin-13 (5nM). Serum deprivation is a specific apoptotic insult; it causes mitochondrial depolarization as shown by decreased TMRM signal. Apelin-13 noticeably prevented the collapse of the mitochondrial membrane potential. **D**. The bar graph summarizes TMRM fluorescence measurements. Apelin-13 maintained the mitochondrial membrane potential at normal levels. N = 5 independent assays, *. $P < 0.05$ compared with SD (second column). All values of bargraphs in this figure and following figures are mean ± SEM.

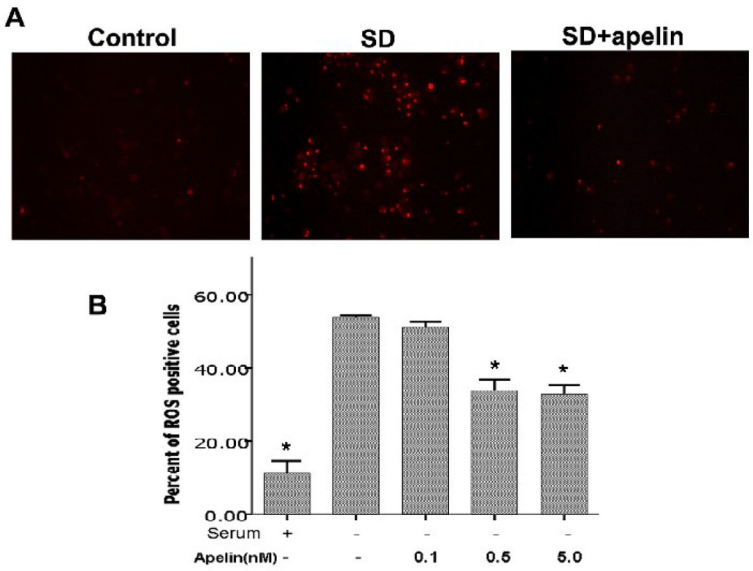

Figure 3. Effects of apelin-13 on serum deprivation-induced ROS production

A. Detection of reactive oxygen species (ROS) in cortical neurons cultures. In control cultures or cultures after 10 hr exposure to SD with or without apelin-13 (5 nM), cells were incubated with DHE for 5 min to detect ROS production. Serum deprivation increased DHE fluorescence while it was significantly reduced by co-applied apelin-13 (0.5 – 5.0 nM). **B**. The bar graph shows the averaged percent of DHE-positive cells to total cells labeled with Hoechst 33342 (not shown). N = 3;*. $P < 0.05$ compared with SD (second column).

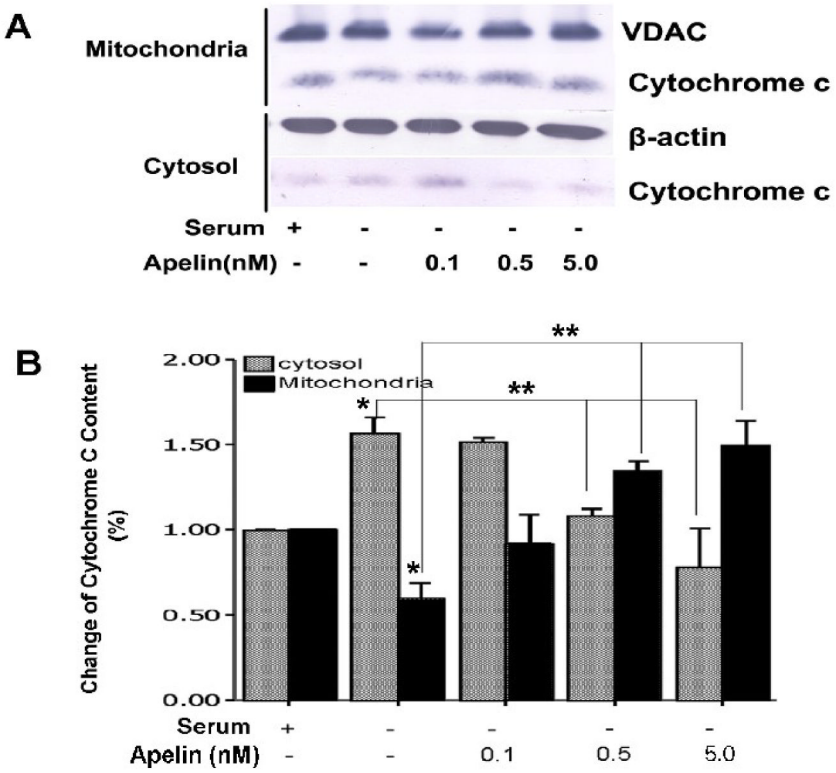

Figure 4. Effect of apelin-13 on serum deprivation-induced cytochrome c release

Cytochrome c content in mitochondria and cytoplasm compartments was evaluated using Western blotting. Protein expression was corrected according to the loading control of VDAC and β-actin in mitochondria and cytosolic fractions, respectively. **A**. Western blot gel shows cytochrome c contents in serum and serum free medium, with different concentrations of apelin-13. **B**. Summarized data from experiments in A. Serum withdrawal significantly diminished cytochrome c content in mitochondria while its content increased in cytoplasm. Apelin-13 prevented the cytochrome c translocation. N = 5; *. $P < 0.05$ compared with serum medium control, **. $P < 0.05$ compared with serum-free medium.

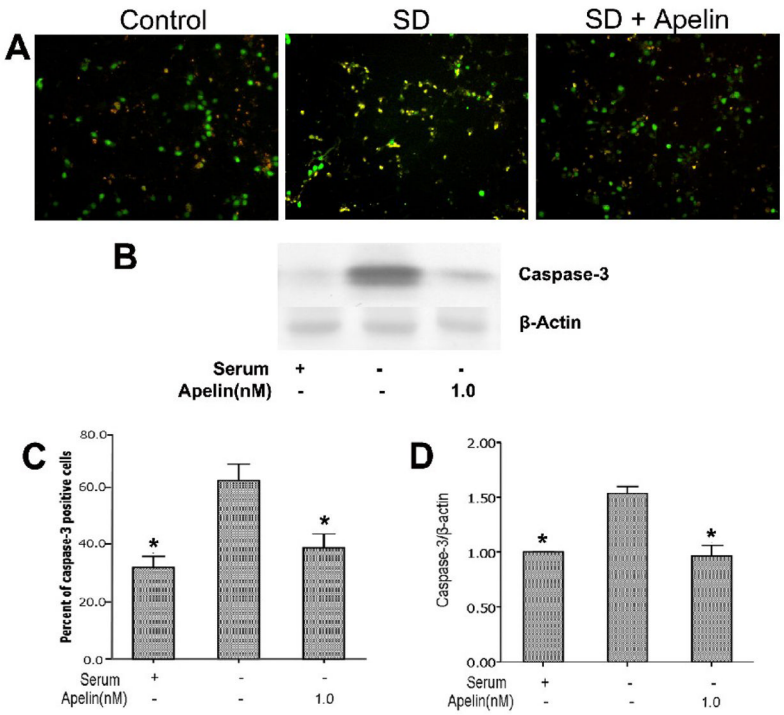

Figure 5. Effects of apelin-13 on serum deprivation-induced caspase-3 activation

Cortical neurons were treated with serum deprivation for 16 hours. Caspase-3 activity was determined using an antibody against cleaved caspase-3. **A**. Caspase-3 staining showed increased caspase-3-positive cells, apelin-13 (5 nM) inhibited caspase-3 activation. **B** . Percentage of caspase-3 positive cells summarized in the bargraph. N = 3 independent assays; *. $P < 0.05$ compared to SD alone. **C**. Cell lysates were analyzed for cleavage of caspase-3 by Western blotting. SD markedly increased cleaved caspase-3 and this increase was prevented by apelin-13 (1 nM). **D**. Average values of gray intensity of the Western blot analysis. N = 3; *. $P < 0.05$ vs. SD alone.

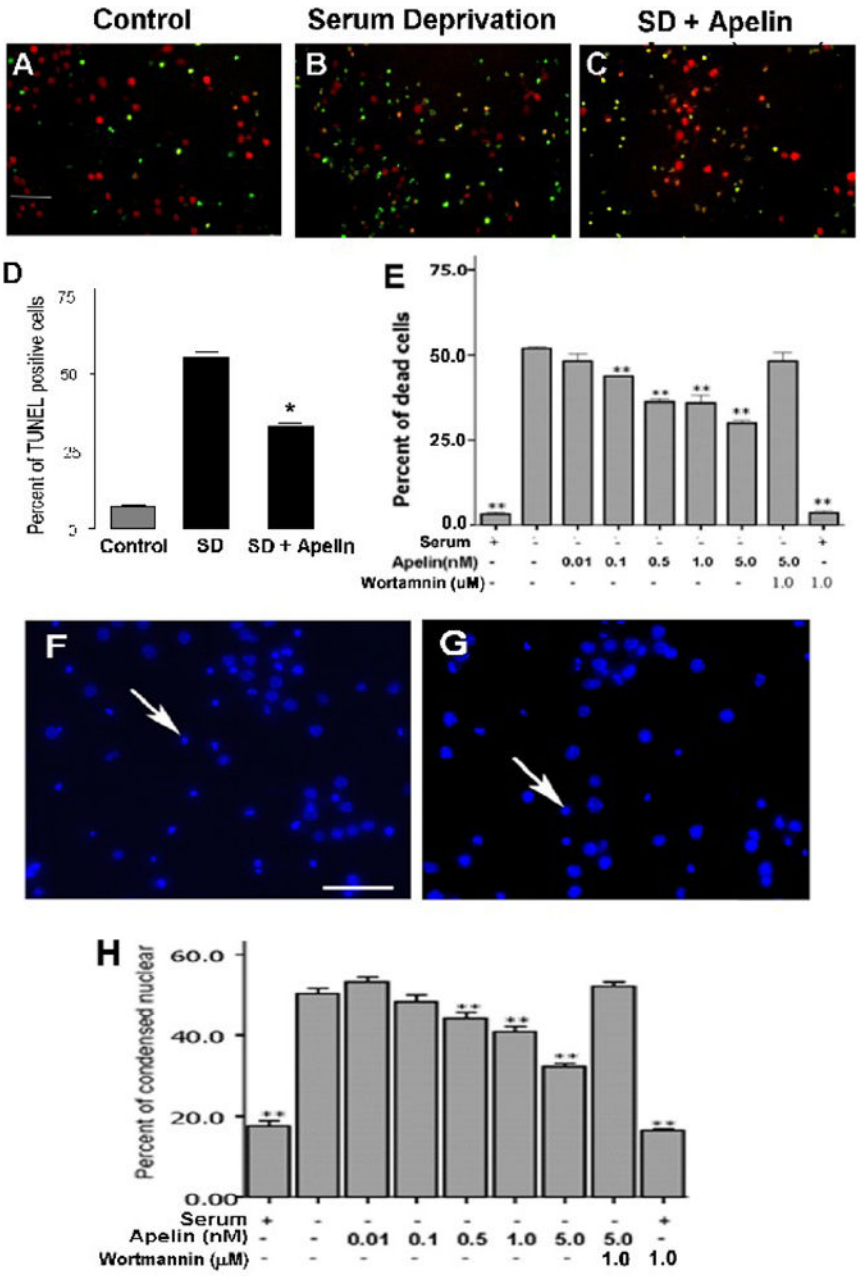

Figure 6. Apelin-13 protective effect against serum deprivation induced cell death

In cortical cultures, apelin-13 was neuroprotective against serum deprivation-induced cell death. **A - C**. Mouse cortical cultures were treated with serum deprivation for 24 hrs with or without co-applied apelin-13. Cells were then stained with TUNEL to detect DNA damage of dying/dead cells (green). Neurons were labeled with NeuN (red). Serum deprivation caused noticeable cell shrinkage (also see F and G). **D.** Summarized data of immunocytochemical detection of TUNEL-positive cells. Apelin (5 nM) reduced the percentage of TUNEL-positive cells 24 hrs after serum withdrawal. **E.** Apelin-13 dose-dependently attenuated serum deprivation-induced neuronal cell death. The protective effect was blocked by the PI3/Akt signaling inhibitor wortmannin (1.0 μM). Wortmannin alone did not cause cell death. **F** and **G** . Hoechst 33342 staining labeled cell nuclei, condensed

Hoechst staining was suggestive of shrunken cells (arrow). Apelin (5 nM) treatment (G) attenuated the number of shrinking cells and extent of cell shrinkage after 24-hr serum deprivation (F). **H**. Summary of cell counts of condensed nuclear. Apelin dose-dependently prevented cell shrinkage. The effect was blocked by wortmannin (1 μM). N = 3 independent assays; *, **. $P < 0.05$ vs. SD alone.

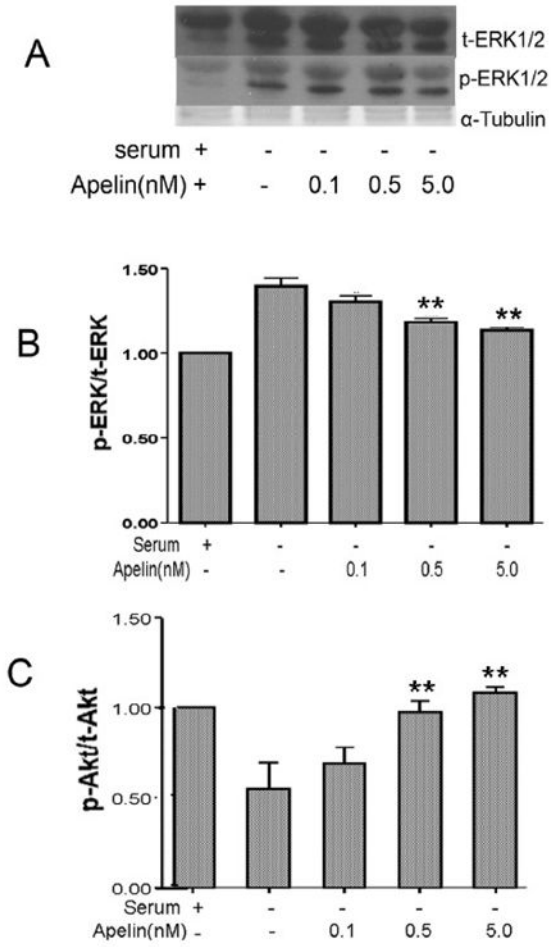

Figure 7. The role of ERK1/2 and PI3/Akt pathways in apelin effect

Cortical cultures was treated with serum deprivation for 4 hrs with or without apelin-13 (0.1 – 5.0 nM) and Western blot was analyzed for phosphorylated ERK and Akt. **A**. Western blotting of phosphorylated ERK(p-ERK) and total ERK expression under different conditions. **B**. Densitometry of p-ERK/t-ERK levels normalized to α-tubulin for each treatment condition in A. Serum deprivation enhanced p-ERK level and apelin dose dependently decreased the ERK phosphorylation. N = 3; *. P < 0.0 5 vs. SD alone. **C**. Expression of phosphorylated Akt (p-Akt) in cortical neurons. Densitometry of p-Akt/t-Akt normalized to α-tubulin showed that serum deprivation attenuated p-Akt, this reduction was overcame by co-applied apelin-13 in a dose-dependent manner (0.1 – 5 nM). N = 3, **. P < 0.01 vs. SD alone.

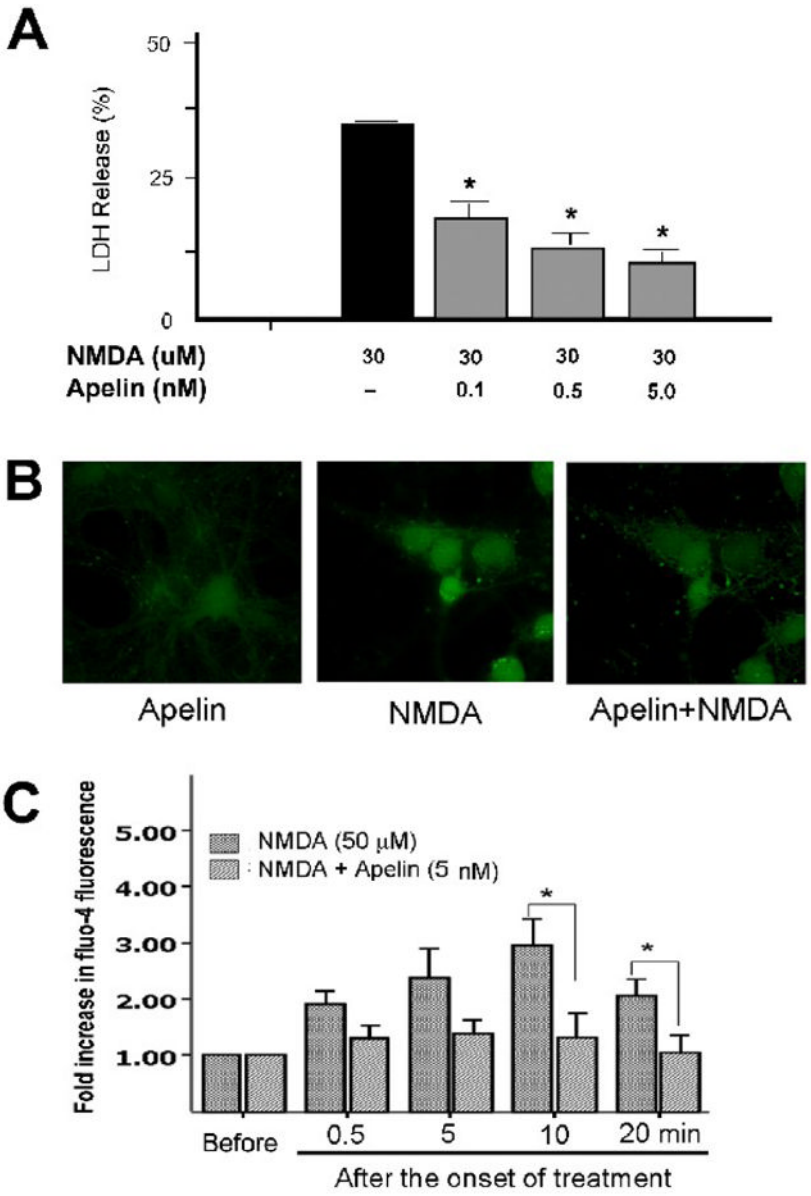

Figure 8. Protective effect of apelin-13 against NMDA-induced excitotoxicity

Cortical cultures were subjected to NMDA exposure of excitotoxic insult. Cell death and Ca^{2+} increases were measured. **A**. Cortical neurons were treated with 30 μM NMDA for 24 hrs with or without apelin-13 (0.1 – 5 nM). LDH release in the medium was detected and normalized with total kill (300 μM for 24 hrs) N = 3 assays. Apelin-13 decreased LDH release in a dose dependent manner. *. $P < 0.05$ vs. NMDA group. **B**. Apelin-13 eliminated NMDA-induced Ca^{2+} accumulation in cortical neurons. Apelin-13 (5 nM) was added 5 min before NMDA (50 μM). Fluo-4 fluorescent imaging of similar populations of cells taken 20 min after NMDA application, showing significant increase of cellular Ca^{2+} in cortical neurons. Apelin-13 significantly prevented the NMDA-induced Ca^{2+} increase. **C**. Fluo-4 imaging was taken at different times after treatments. The intensity of the fluorescence was quantified using image J software. Apelin-13 (5 nM) prevented the NMDA-induced Ca^{2+} increases after different time points after NMDA exposure. Apelin-13 (5 nM) alone did not change intracellular Ca^{2+} for up to 20 min. N = 3 experiments. *. $P < 0.05$ vs. NMDA group.